

Curling spin density and orbital structures in a magnetic vortex core of an Fe quantum dot

Kohji Nakamura* and Tomonori Ito

Department of Physics Engineering, Mie University, Tsu, Mie 514-8507, Japan

A. J. Freeman

Department of Physics and Astronomy, Northwestern University, Evanston, Illinois 60208, USA

(Received 4 June 2003; published 14 November 2003)

First results of the spin and orbital structures in the vortex core of an Fe dot obtained using highly precise first principles calculations that include intra-atomic noncollinear magnetism are reported. We demonstrate that a curling magnetic structure is stabilized within a 4 nm radius dot as inferred from spin-polarized scanning tunneling microscopy experiments in which the spin directions close to the center of the dot turn up along the perpendicular orientation to the curling plane—and also predict a complicated curling intra-atomic noncollinear magnetism near the center in which the spin moments continuously cant in circular directions on a smaller length scale inside the atoms. Importantly, these rotation properties in the spin density couple to the orbital motion and induce orbital moments oriented perpendicular to the curling plane, which is a first prediction of quantum phenomena induced in the nanoscale vortex core.

DOI: 10.1103/PhysRevB.68.180404

PACS number(s): 75.75.+a, 73.21.La, 75.50.Tt

In ferromagnetic dot nanostructures,^{1,2} which are promising candidates for nonvolatile memory applications, curling magnetic structures that determine their properties are known to form in order to reduce the demagnetization energy of the dot volume. However, the magnetization close to the center of the dot, the so-called singular (or Bloch) point, cannot remain circular because the short-range exchange interaction energy becomes dominant; thus, to avoid the singularity, the magnetization is expected to turn up along the perpendicular orientation. Understanding the nature of the Bloch point, which is thought to spatially link classical and quantum magnetism,² represents a severe challenge. The characteristic length resulting from the competition of the exchange and dipole-dipole interactions, defined as $\xi_{ex} = \sqrt{A/K_d}$, where A is the exchange stiffness constant and K_d is the stray field energy density, is only of the order of nanometer for soft magnetic materials,¹ e.g., 5 nm for permalloy and 3 nm for Fe. Hence, the ground state of the vortex structure appears to be governed by atomic-scale considerations and needs to be treated with quantum mechanics.

Experimentally, the magnetic vortex structures inferred using holographic interference electron microscopy,³ and recent magnetic force microscopy (MFM) investigations⁴ provided clear evidence of the vortex core structures in which the magnetization near the center assumes a perpendicular orientation. Furthermore, spin-polarized scanning tunneling microscopy (SP-STM) (Ref. 5) observed that the core structures were confined to a 4 or 5 nm radius, which is comparable with the above characteristic length.

Aside from these investigations, little is so far known about their electronic and magnetic structures based on quantum mechanics. Here, we investigate the vortex core structure in an Fe dot from first principles, using the highly precise full-potential linearized augmented plane-wave (FLAPW) method⁶ including noncollinear magnetism at the electronic scale with no shape approximation to the spin magnetization density,⁷⁻⁹ and demonstrate how the spin magnetization near the Bloch point turns up along the per-

pendicular orientation to the curling plane in which, we find that the rotation properties in the spin density couple to the orbital motion and induce orbital magnetic moments orienting along the perpendicular direction. These predictions invite experimental confirmation, possibly with magnetic circular dichroism, hyperfine interaction, or neutron measurements.

In noncollinear magnetic systems, such as vortex structures where a spatial variation of the magnetization orientation is allowed over all space, the electron density and the effective potential in density-functional theory¹⁰⁻¹² are treated with a 2×2 density matrix $\rho(\mathbf{r}) = \rho_0(\mathbf{r})\mathbf{I} + \mathbf{m}(\mathbf{r}) \cdot \boldsymbol{\sigma}$ and the effective potential matrix $\mathbf{V}_{\text{eff}}(\mathbf{r}) = V_0(\mathbf{r})\mathbf{I} + \mathbf{V}_m(\mathbf{r}) \cdot \boldsymbol{\sigma}$, where \mathbf{I} and $\boldsymbol{\sigma}$ are the unit matrix and Pauli spin matrix, respectively, and $\rho_0(\mathbf{r})$ and $\mathbf{m}(\mathbf{r})$ correspond to a charge density and a magnetization density. The $\mathbf{V}_{\text{eff}}(\mathbf{r})$ contains a nonmagnetic part $V_0(\mathbf{r})$ and a vector magnetic part $\mathbf{V}_m(\mathbf{r})$, which are given by external, Coulomb and exchange-correlation potentials. The potential is represented within the full-potential scheme prescribed by Weinert¹³ and applied in the local spin-density approximation (LSDA) using the von Barth-Hedin exchange correlation.¹⁰ The basis functions are specified with the spin-independent LAPW basis^{8,9} in order to avoid discontinuity in augmentation of the basis functions at the muffin tin (MT). The diagonalization is carried out in the whole spin space since spin-up and spin-down wave functions are no longer independent. Now the calculations require full self-consistency for the density matrix, i.e., the magnetization direction as well as the magnitude is determined self-consistently.

As a model of the dot shown in Fig. 1, we employed a repeated disk structure (rod) with 29 Fe atoms in a unit cell; the rods are placed on a square lattice separated by vacuum regions with $5\sqrt{2}a$, where a is the experimental lattice constant of bulk bcc Fe. The self-consistent LSDA calculations were performed with the scalar relativistic corrections, i.e., excluding the spin-orbit coupling (SOC) (Ref. 14) without any constraints except that the spin magnetic orientations in

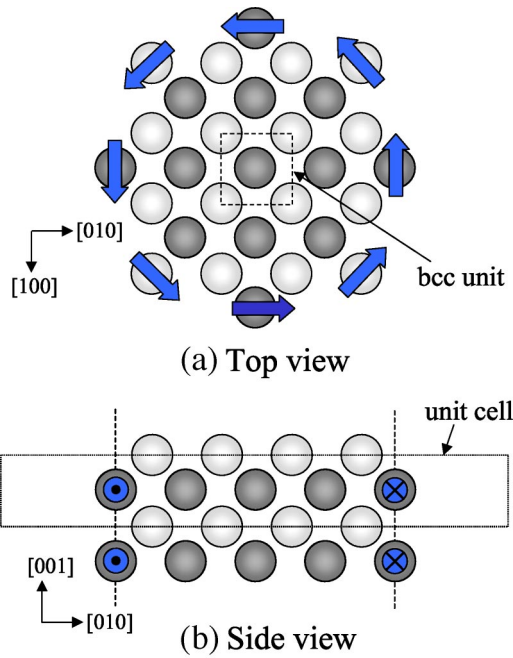


FIG. 1. (Color online) Model of the disk/rod structure employed: (a) top view, (b) side view. Light and dark circles indicate atoms on alternating (002) planes.

the outer atoms of the disk are fixed along the tangential directions. As a reference, we performed self-consistent LSDA calculations for a system without the vortex [i.e., a collinear ferromagnetic (FM) dot] with the same lattice and computational parameters.

The spatial distribution of the calculated spin magnetization $\mathbf{m}(\mathbf{r})$ and the integrated out-of-plane components in the MT spheres, $M_{\perp} = \int_{\text{MT}} \mathbf{m}_{\perp}(\mathbf{r}) d\mathbf{r}$, are shown in Figs. 2 and 3 (with solid circles), respectively. The spin moments aligning almost collinearly at each atom are localized near the nucleus, and clearly orient in the tangential directions around the center of the dot. Upon moving to the center, the in-plane components gradually decrease while the out-of-plane components increase, so that the spin directions continuously turn up along the perpendicular orientation to the curling plane, as predicted from classical micromagnetic calculations.^{1,4}

By forming the vortex core, the magnitude of the spin moments is reduced, however, from that in the FM dot as a result of changes in the electronic structure: Fig. 3 (open circles) shows the difference in magnitude of the total moments in the MT spheres between systems with and without the vortex core, ΔM . The reduction of the moments in the center region reaches the sizeable value of $0.14\mu_B$.

Furthermore, a rather complicated pattern of the spin magnetization density is found near the center in which the moment directions vary continuously on a smaller length scale inside the atoms. Figure 4 shows the in-plane components $\mathbf{m}_{\parallel}(\mathbf{r})$ of the spin magnetization density on (a) the (001) plane through the nucleus of the center atom, on parallel planes (b) $\frac{1}{20}a$ ($a = \text{bcc lattice constant}$) and (c) $\frac{1}{10}a$ above the nucleus. Surprisingly, the spin moments in the outer portions directed toward the nearest-neighbor Fe at-

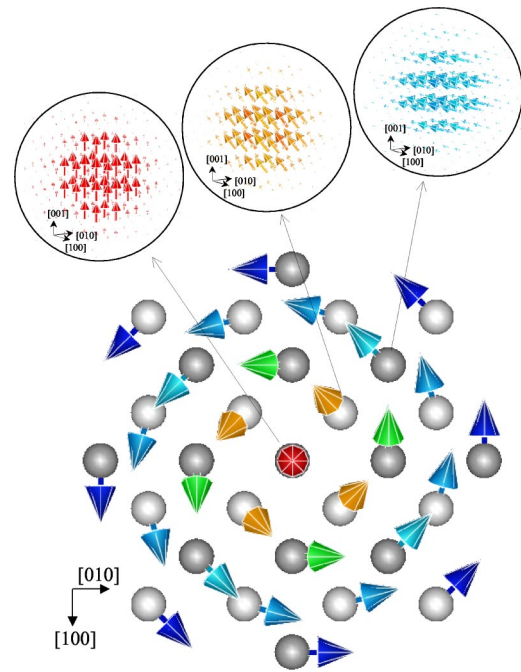


FIG. 2. (Color online) Spatial distribution of the calculated spin magnetization density, $\mathbf{m}(\mathbf{r})$, in a magnetic vortex Fe dot. The large arrows on the atom sites show the average direction in the MT spheres, which turns up along the out-of-plane orientation (represented by red arrows) from the in-plane orientation (blue arrows), on moving to the center of the dot. The blow-ups show details of the intra-atomic spin-density distributions on selected sites.

oms, which directly hybridize with $d_{xz,yz}$ orbitals, are predicted to curl in a counterclockwise direction, while those near the nucleus cant in the opposite (clockwise) direction [c.f. Fig. 4(a)]. An oppositely directed curling spin density is also found throughout the outer interstitial region due to the negative polarization of the delocalized s and p electrons,¹⁵ but with a very small moment.

The formation energy of the vortex core, ΔE_{vc} , calculated as the total energy difference from that of the FM dot state, is found to be 88 meV/cell (3 meV/atom)—which roughly corresponds to the demagnetization energy of a 4 nm

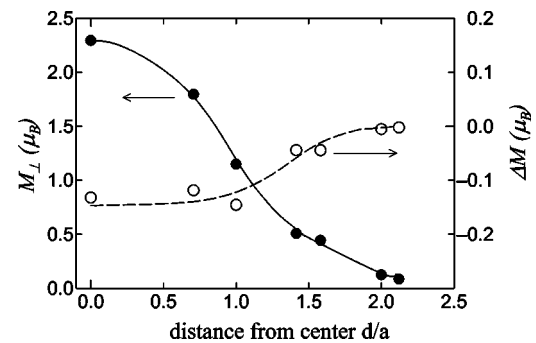


FIG. 3. Out-of-plane components of spin moments inside the muffin-tin spheres, M_{\perp} , and the difference in the magnitude of the total moments in the MT spheres between systems with and without the vortex core, ΔM , as a function of the distance d/a from the center of the dot, where a is the bcc lattice constant of bulk Fe.

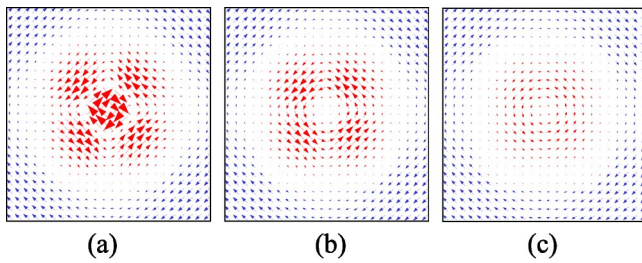


FIG. 4. (Color online) In-plane components of magnetization densities, $\mathbf{m}_{\parallel}(\mathbf{r})$, on (a) the (001) plane at the center atom, on parallel planes (b) $\frac{1}{20}a$ (a is the bcc lattice constant) and (c) $\frac{1}{10}a$ above the nucleus, where the magnitude of the moments represented by blue arrows are enlarged three times that of the red arrows. The average moment orients in an out-of-plane direction. The area shown is $a/2 \times a/2$.

radius FM dot found by phenomenological calculations.¹ This may indicate that the vortex core will be stabilized when the radius becomes of this magnitude, which agrees with the SP-STM observations.⁵ In determining these structures more quantitatively, of course, further investigations will be necessary.

The curling of the spin magnetization produces rotation structures in the effective LSDA potential, which lifts the orbital degeneracy and leads to a nonzero orbital angular momentum. Indeed, we observed orbital magnetic moments oriented perpendicular to the curling plane in which no in-plane components were observed. The out-of-plane components of the orbital moments M_{\perp}^{orbit} , calculated within the scalar relativistic approximation without SOC, are shown in Fig. 5 as solid circles. Orbital moments near the center, $0.03\mu_B - 0.06\mu_B$, are clearly induced in the perpendicular orientation to the curling plane. Thus, the rotation properties in the spin density couple to the orbital motion, and may lead to an uniaxial magnetic anisotropy in the perpendicular direction.

Now, when the SOC is introduced, the vortex core structure is stabilized by 1 meV/cell in the ΔE_{vc} ; the spin-density structures are not significantly changed. Since the SOC induces the atomic orbital moments along the spin moment orientations,¹⁶ the orbital moments also curl around the center of the dot, in which the moments turn up along the perpendicular orientation at the center. However, due to the interaction with the curling spin density which induces the

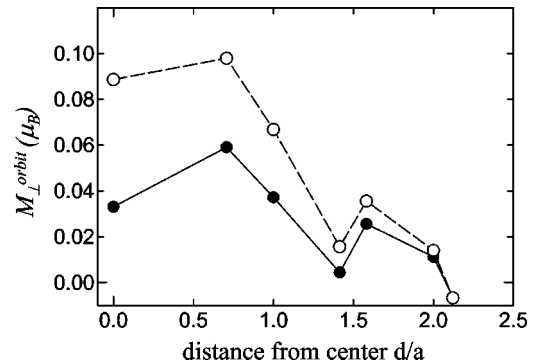


FIG. 5. Out-of-plane components of orbital moments, M_{\perp}^{orbit} , as a function of the distance d/a from the center of the dot. Solid and open circles represent results without and with spin-orbit coupling.

orbital moments along the perpendicular direction, the orbital moments do not coincide with the spin directions. The out-of-plane components are enhanced by about a factor of 2 from the states without SOC, as seen in Fig. 5. The magnitude at the center atom, $0.089\mu_B$, is larger than that in the FM dot, $0.055\mu_B$. The small hump at a distance d/a of 1.5–2.1 is due to the well-known surface effects that enhance the magnitude of the orbital moments.¹⁶

Finally, we comment briefly on the behavior of two vortex states whose spin densities rotate in clockwise and counter-clockwise directions, i.e., right- and left-handed chiral structures. These structures were experimentally confirmed by Lorentz microscopy and the MFM,¹⁷ and the circular direction can be controlled by introducing an asymmetry into the geometrical shape of the circular dot with a field applied in-plane to the dot.¹⁸ Indeed, both energy states are not degenerate since a current field due to a $\nabla \times \mathbf{m}(\mathbf{r})$ term produces a chirality which breaks the symmetry of the two vortex states. While these current effects may be so small that no preferential chirality would appear in say, MFM experiments,¹⁹ their pursuit provides a meaningful and interesting challenge.

We thank R. Wu, M. Weinert, T. Ocuchi, T. Jo, and A. Tanaka for fruitful discussions and suggestions. Computations were performed at the Supercomputer Center, Institute for Solid State Physics, University of Tokyo, and the Cooperative Research Center, Mie University.

*Email address: kohji@phen.mie-u.ac.jp

¹A. Hubert and R. Schäfer, *Magnetic Domains* (Springer-Verlag, Berlin, 1998).

²J. Miltat and A. Thiaville, *Science* **298**, 555 (2002).

³A. Tonomura, T. Matsuda, J. Endo, T. Aarii, and K. Mihama, *Phys. Rev. Lett.* **44**, 1430 (1980).

⁴T. Shinjo, T. Okuno, R. Hassdorf, K. Shigeto, and T. Ono, *Science* **289**, 930 (2000).

⁵A. Wachowiak, J. Wiebe, M. Bode, O. Pietzsch, M. Morgenstern, and R. Wiesendanger, *Science* **298**, 577 (2002).

⁶E. Wimmer, H. Krakauer, M. Weinert, and A.J. Freeman, *Phys. Rev. B* **24**, 864 (1981); M. Weinert, E. Wimmer, and A.J. Free-

man, *ibid.* **26**, 4571 (1982), and references therein.

⁷L. Nordström and D.J. Singh, *Phys. Rev. Lett.* **76**, 4420 (1996).

⁸K. Nakamura, A.J. Freeman, D.S. Wang, L. Zhong, and J. Fernandez-de-Castro, *Phys. Rev. B* **65**, 012402 (2002).

⁹K. Nakamura, T. Ito, A.J. Freeman, L. Zhong, and J. Fernandez-de-Castro, *Phys. Rev. B* **67**, 014420 (2003).

¹⁰U. von Barth and L. Hedin, *J. Phys. C* **5**, 1629 (1972).

¹¹J. Kübler, K.-H. Höck, J. Sticht, and A.R. Williams, *J. Phys. F: Met. Phys.* **18**, 469 (1988).

¹²L.M. Sandratskii, *Adv. Phys.* **47**, 91 (1998).

¹³M. Weinert, *J. Math. Phys.* **22**, 2433 (1981).

- ¹⁴D.D. Koelling and B.N. Harmon, *J. Phys. C* **10**, 3107 (1977).
- ¹⁵S. Ohnishi, A.J. Freeman, and M. Weinert, *Phys. Rev. B* **28**, 6741 (1983).
- ¹⁶R. Wu and A.J. Freeman, *J. Magn. Magn. Mater.* **200**, 498 (1999).
- ¹⁷J. Raabe, R. Pulwey, R. Sattler, T. Schweinböck, J. Zweck, and D. Weiss, *J. Appl. Phys.* **88**, 4437 (2000).
- ¹⁸M. Schneider, H. Hoffmann, and J. Zweck, *Appl. Phys. Lett.* **79**, 3113 (2001).
- ¹⁹T. Okuno, K. Shigeto, T. Ono, K. Mibu, and T. Shinjo, *J. Magn. Magn. Mater.* **240**, 1 (2002).